www.czasopisma.pan.pl PAN www.journals.pan.pl

ARCHIVES of FOUNDRY ENGINEERING

VERSITA

DOI: 10.2478/v10266-012-0070-5

Published quarterly as the organ of the Foundry Commission of the Polish Academy of Sciences

ISSN (2299-2944)
Volume 12
Issue 2/2012

261 – 266

Microstructure and Microhardness of Ti6Al4V Alloy Treated by GTAW SiC Alloying

W. Bochnowski*
Institute of Technics, Rzeszow University, Rejtana 16 C, 35-310 Rzeszow, Poland
*Corresponding author. E-mail address: wobochno@univ.rzeszow.pl

Received 25-05-2012; accepted in revised form 31-05-2012

Abstract

In this work, the change of the structure and microhardness of Ti6Al4V titanium alloy after remelting and remelting with SiC alloing by electric arc welding (GTAW method) was studied. The current intensity equal 100 A and fixed scan speed rate equal 0,2 m/min has been used to remelting surface of the alloy. Change of structure were investigated by optical and scanning electron microscopy. Microhardness test showed, that the remelting of the surface does not change the hardness of the alloy. Treated by GTAW SiC alloying leads to the formation of hard (570 HV0, 1) surface layer with a thickness of 2 mm. The resulting surface layer is characterized by diverse morphology alloyed zone. The fracture of alloy after conventional heat treatment, similarly to fracture after remelting with GTAW is characterized by extremely fine dimples of plastic deformation. In the alloyed specimens the intergranular and crystalline fracture was identified.

Keywords: Titanium Alloy, Arc Plasma Treatment, Alloying, Structure, Fracture, Microhardness

1. Introduction

Two phase α+β titanium alloys are widely used in aerospace, chemical, energy automotive industry also two phase titanium alloys are effectively applied on medical implant. One of the very popular titanium alloys (the 60% total USA titanium alloy market) for these applications is Ti6Al4V (ASTM – Grade 5) [1]. The most important characteristic features of this alloy are low density 4.42 g/cm^3 associated with a high melting point 1649°C, high strength (1000 MPa tensile strength) and high corrosion resistance. However, the relatively low microhardness and high friction coefficient of around 0.8 lead to decreases the tribological properties of the alloy. To improve his microhardness and wear resistance, are subjected to advanced surface treatments [2, 3].

One of the treatments is remelting of the surface layer by the source of concentrated energy (laser, electron beam or arc plasma) in atmosphere of reactive gases as well as application o the concentrated energy sources to the introduction in the area of liquid metal, elements and compounds alloying [4, 5, 6, 7]. The melting pool was cooled by the shielding gas and the conduction of heat through the substrate.

In article [8] were presented the investigations results of titanium alloy Ti6Al4V surface layer after laser melting process. The process of laser melting was performed using Nd-YAG laser with different scanning speeds and different shifts in the laser beam. It was showed that laser melting process leads to increases of wear resistance. The authors in work [9] showed that the remelting hardening with gas tungsten arc welding (GTAW) method of the surface of Ti6Al4V titanium alloy caused rise in microhardness in the case of applied current in range 10-40A and voltage 12-15V. They obtained a highest hardness on the level of 550 HV 0,1. Authors of work [10] have used pulsed laser to modifications surface of Ti6Al4V with SiC. Authors exhibit that

obtained surface layers (about maximum depth 0,15 mm) have higher microhardness (5-6 GPa) about 50 % in relation to the substrate and very good wear resistance. The experimental results of authors of work [3] show that the SiC clad layer specimen (with GTAW method) under a dry sliding wear test condition exhibited better wear performance than that of the un-clad Ti–6Al–4V alloy specimen.

The aim of the work was to determine the effect of SiC alloying on the changes structure microhardness and fracture topography of Ti6Al4V titanium alloy. The alloying layers were produced using the GTAW method.

2. Material and methodology

The material investigated was a Ti6Al4V alloy, of composition 6,75 Al; 4,15 V; 0,27 Fe; 0.32 Si; 0,029 Cr, 0,062 Zn, (in %wt).

The alloy treated at 925°C for 1 hour, air cooled and then stabilized at 700°C for 2 hours. The microstructure of this alloy is shown in Fig. 1. The structure is two-phased, consists of α and β solid solution. The samples with dimensions 30 mm x 30 mm were cut from a 5 mm thick sheet. On the surface of alloying specimens (8 mm x 30 mm) were made holes about 1 mm diameter and 1 mm depth. Distance between the holes (in two perpendicular directions) was equal 1 mm. Next the holes were filled silicon carbide. Silicon carbide crystals had irregular shape (Fig. 2.), their diameter ranged 3 – 15 μm.

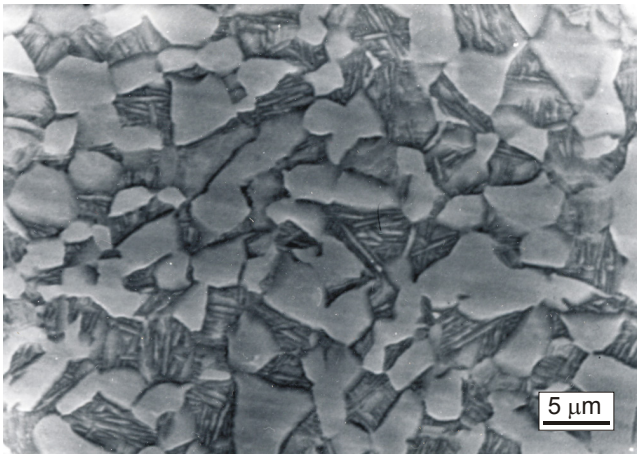

Fig. 1. Structure of the Ti6Al4V alloy after conventional heat treatment, substrate (SUB), light – α phase, dark – β phase. Inside of the dark grain plates α phase are visible

Prepared surface were remelted with gas tungsten arc welding method used. In this experiment a THF 270 A conventional DC Tig welder was used. The parameters of the cladding process were set to weld voltage V=15 V, weld current A=100 A (DC). Scan speed rate was fixed and was equal 0,2 m/min. The diameter of tungsten electrode was 1,6 mm and distance between surface and tungsten electrode tip was 1,5 mm.

The Vickers microhardness tests were performed on cross section of examined specimens by a Hanemann microhardness tester using a load of 100 g. Measurements were made perpendicular to the surface on the three paths in the central zone of the weld. Distance between tracks was 200 μm. The microstructure of metallographically ground, polished and etched samples was investigated using optical (Neophot, Nikon) and scaning electron microscopy (Tesla). The etching agent was 6% vol. HNO_3 and 3% vol. HF in H_2O.

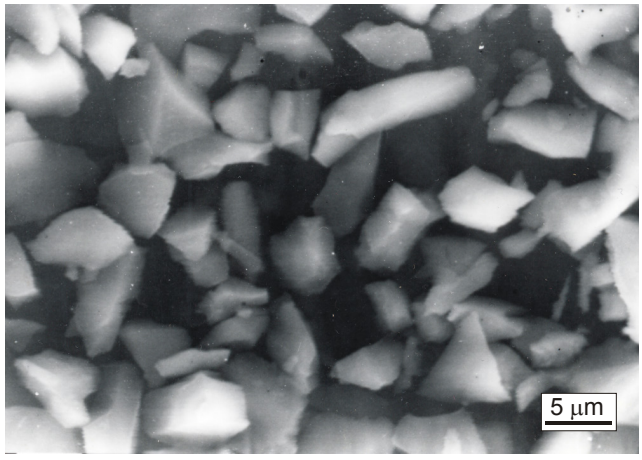

Fig. 2. Silicon carbide particles

3. Results

Microstructure after remelting

Cooling from the liquid state, the Ti6Al4V first traverses the β bcc phase arriving below 1000°C the extensive α + β phase field. The cross section of the titanium alloy after remelting exhibit two areas where structure was changed Fig. 3.

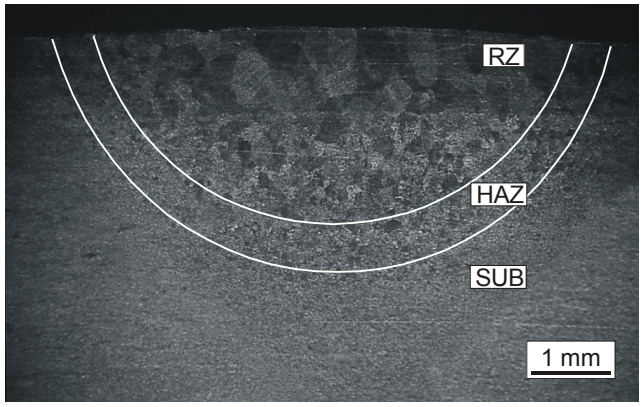

Fig. 3. Optical image of the cross section of the Ti6Al4V after arc plasma treatment. RZ – remelted zone, HAZ - heat affected zone, SUB – substrate

First area – remelted zone (RZ) with a maximum depth 2,5 mm consist of different diameter grain of prior β phase. Near surface remelting the grain had an elongated shape, the diameter

of the grain was about 440 μm. Diameter of the grain decreased in the direction of substrate, as shown in Fig. 4. Bottom remelted zone the diameter of grain was average 50 μm. The microstructure of grains at the top of remelted zone is shown in Fig. 5a. As a result of fast cooling an α phase titanium (shown light) structure was formed in matrix of β metastable solution. The plates of α phase are thin, have less than 1 μm thick.

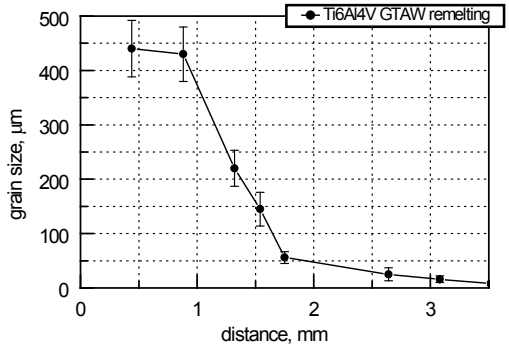

Fig. 4. Grain size of prior β phase in remelted zone

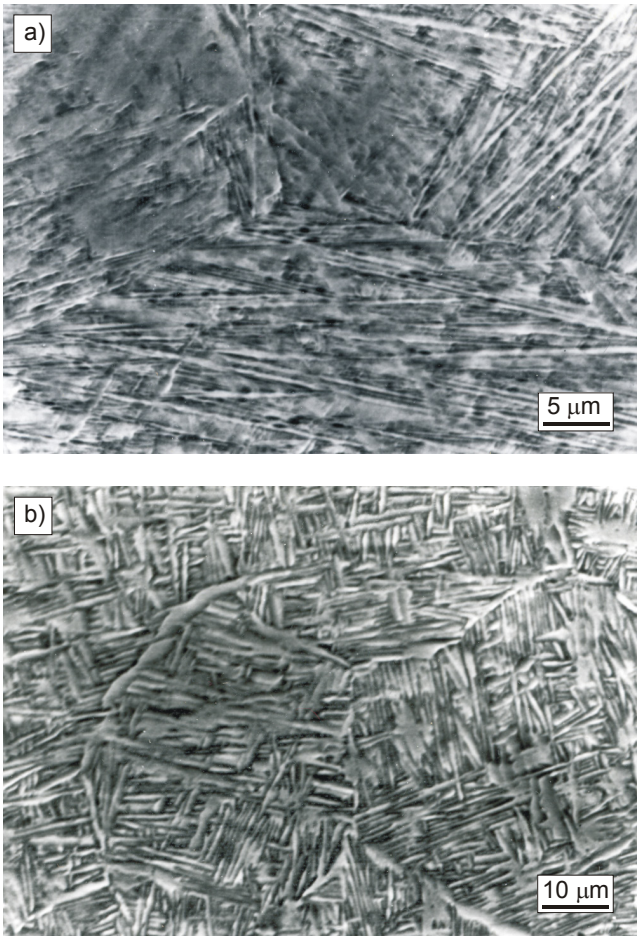

Fig. 5. Remelted zone, a) the grain boundaries of prior α phase is visible, b) bottom structure of RZ

Following the fast cooling no deposition of grain boundary α was recognized. In the bottom of RZ where cooling rate was lower, on the borders of prior β grains an α grain boundary are formed (Fig. 5b). Inside of the grain of prior β phase are visible colony or basket weave of lamellar structures α + β, α - shown light , β - shown dark. The bottom region of the GTAW treatment is dominated by colonies of lamellae starting at grain boundaries. The value and gradient of temperature and slow cooling rate, no influenced on the explicit change of the microstructure in the second area - HAZ (heat affected zone). The microstructure on the border RZ and HAZ is shown in Fig. 6. Microstructure of HAZ is similar to the microstructure of substrate, consist of colonies of primary α and lamellar α+β, with an average grain size of less than 10 μm.

Fig. 6. Microstructure on the border RZ and HAZ

Structure after SiC alloying

View of surface and cross section of the specimens SiC alloyed was shown in Fig. 7.

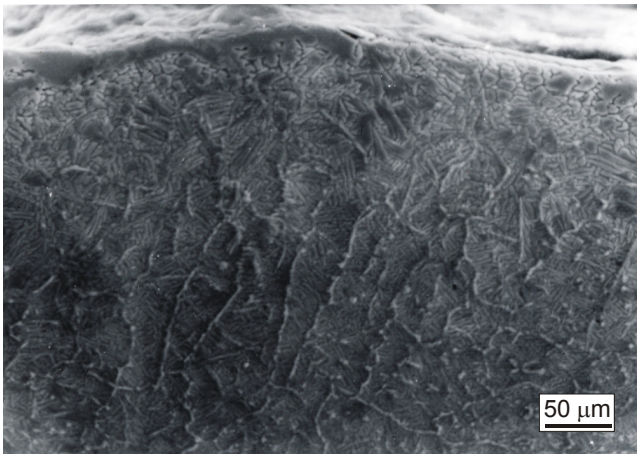

Fig. 7. Microstructure of alloyed zone after GTAW modification with SiC

After GTAW alloying, the alloyed zone about a 2,5 mm of depth (similarly as depth of remelting zone) was obtained. In this zone the investigation of the microstructure showed the columnar and dendritic cells crystals, that were formed during crystallization. The crystals had maximum diameter of 40 μm. Inside of the crystals, products of transformation β → α+β are visible. The parallel bands of plates of the α and β phase no starting at grain boundaries. The lamellae are surrounded by the β phase. The space between the columnar crystals and dendritic cells is filled by carbide phase (most probably SiC ,TiC, Ti_3SiC_2, of eutectic nature [10]), Fig. 7. The SiC particles are practically completely dissolved in remelted area. Occasionally, particularly in the places where were located holes filled by SiC particles, after remelted the dendrites of carbides phases are visible (Fig. 8). The matrix of the area consist of α phase and metastable β phase. Plates of α phase have a irregular shape, their width is more than 3 μm.

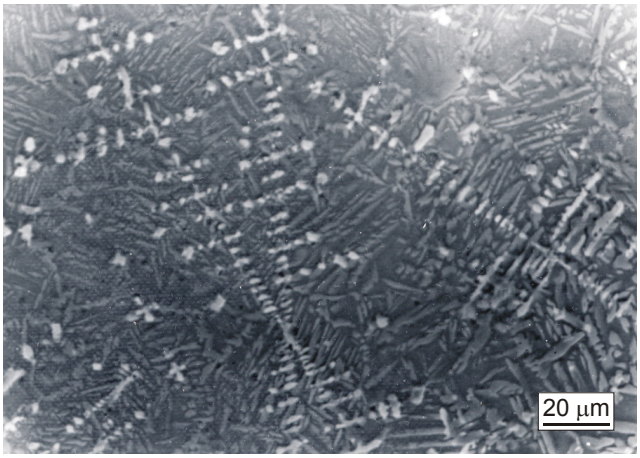

Fig. 8. Microstructure of alloyed zone after GTAW modification with SiC, bright - dendrites of carbides phases

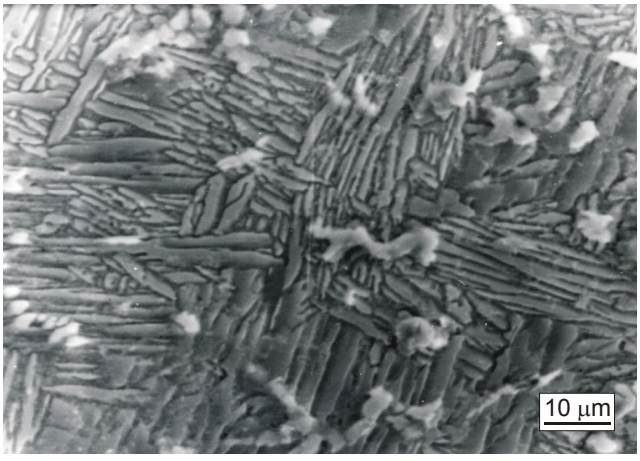

Fig. 9. Microstructure of alloyed zone after GTAW modification with SiC, bright - carbides phases, gray – α phase, black - β phase

In area with a lower content of SiC carbide in the structure was observed carbides, which have irregularly shape and size (size of the carbide was in range 3-15 μm), Fig. 9. These carbides solidified as the first of the liquid. Matrix of the carbides consists of the plates α phase and β phase. Plates α phase (light on Fig. 9) and β phase (dark on Fig. 9) have varied size and are arranged in colonies. Visible in the colonies coarse plates of α phase, have thickness of 4 μm and 15 μm in length. In the structure of the zone alloyed with SiC did not occur the needles of α phase, which were identified in remelting zone of specimens treated by GTAW. For all examined specimens after remelted and alloyed with SiC, no cracking occurred.

Microhardness

The microhardness HV0,1 of the remelting zone and of the alloying zone in dependence on the depth is shown in Fig. 10.

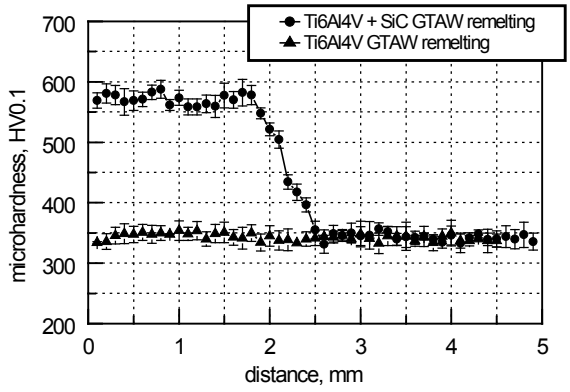

Fig. 10. Microhardness HV0,1 of the Ti6Al4V after remelting and alloying by arc plasma treatment

For the remelting, lower values (330 HV0,1) are recorded near the surface remelted (at a depth of to 200 μm), then the hardness in RZ, HAZ and SUB is maintained at a constant level – 350HV0,1. The hardness depends on the cooling rate, which is determined by the process parameters. In the literature [11] depending on process parameters remelting (at higher cooling rate) an increase of hardness in the RZ and HAZ of was recorded. Performance of SiC alloying resulted in increase of hardness in the alloyed zone. The difference in hardness between the alloyed zone and the base metal is 220HV0,1.

The increase of hardness effect has been reported by [12]. The Authors obtained an increase of 300 HV0,1 Ti6Al4V alloy of SiC clad layer. The increase of hardness was explained a high proportion of carbide phase (TiC, Ti_8C_5, VC) in the formed layer. Alloying with SiC by GTAW clearly enhanced the wear resistance of the Ti6Al4V alloy.

On the bottom alloyed zone and in border of zone alloyed and HAZ (on the 500 mm length) a continuous decline of the hardness was showed in fig 10. The hardness HAZ in alloyed specimens was on level hardness of substrate.

Fracture topography

For assess the impact of treatment on the type of fracture, the specimens were prepared by making the V-notch at the center of the weld metal and a broken by Charpy hammer. The Ti6Al4V alloy (after conventional heat treatment) fracture was found to be associated with more number of voids. On the Fig. 11 we can see network of extremely fine dimples in the relatively flat areas. The dimple size appears to be orientation dependent.

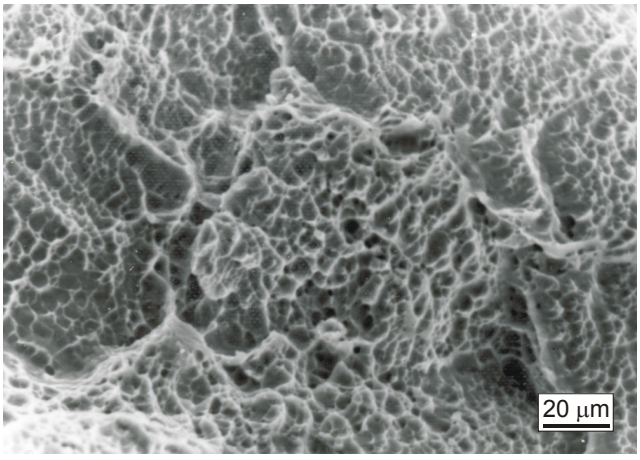

Fig. 11. The Substrate. The network of extremely fine dimples of plastic deformation in the Ti6Al4V after conventional heat treatment

Generally, fracture of remelted specimens was similar to substrate fracture. Occasionally the fracture surface in RZ has higher roughness. Locally, in the central area of RZ, the intergranular fracture is visible. The fracture appeared to take place at the prior β grain boundaries, (Fig. 12).

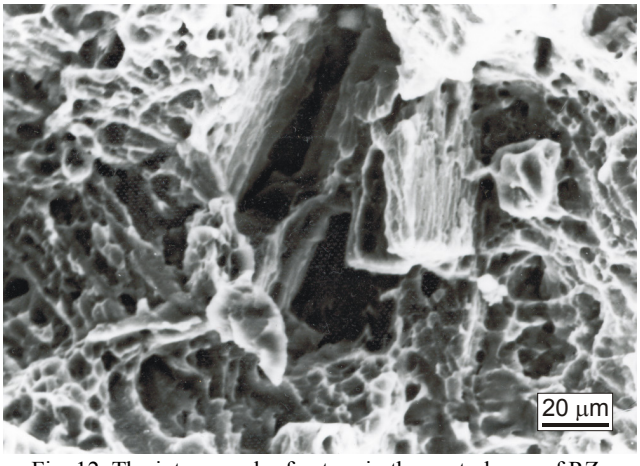

Fig. 12. The intergranular fracture in the central area of RZ

Microstructure on the alloyed zone has a very high hardness, which is usually associated with a loss in fracture toughness. Fracture toughness of titanium alloys is very dependent on microstructural and also crystallographic characteristics In the alloying zone, the intergranular and transcrystalline fractures were observed. Near treated surface (to 400 mm of depth) on the border of dendrite of prior β phase the intergranular fracture was dominated. The cleavage plane passing between the plates of α and β phases is shown in Fig. 13.

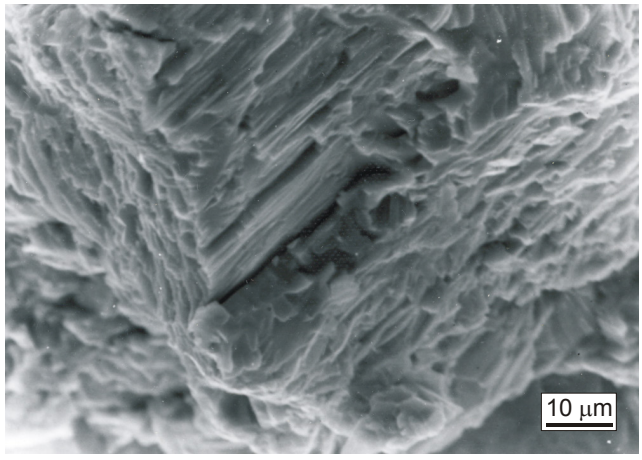

Fig. 13. Intergranular fracture of the alloyed specimen. The crack between the plates of α phase is visible

Below, in the alloying zone has performed relatively flat, transcrystalline fracture, with less roughness compared to the roughness of fracture near surface treated. The transcrystalline failure is due to the separation in α plate interfaces, Fig. 14. The lamellar microstructure induces crack deviations and bifurcations following colony boundaries.

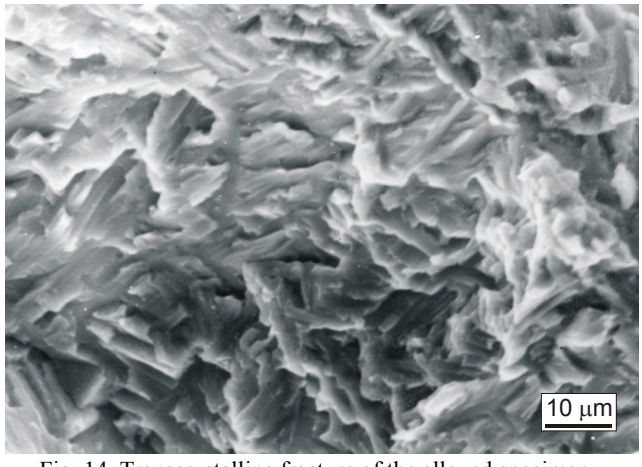

Fig. 14. Transcrystalline fracture of the alloyed specimen. The bootom the crack between the plates of α phase is visible

4. Conclusions

GTAW treatment can be competitive compared to other methods that use a concentrated source of energy to the process of alloying surface. Alloying of Ti-6Al-4V alloy led to improvement of microhardness for the applied process parameters of remelting. The alloying layer do not reveal cracks. Microhardness of substrate amounted to about 350HV0.1. Alloyed with SiC increased the microhardness of surface layer to 570HV0,1. Depending on the volume of SiC introduced into the molten weld pool was observed structures: the grid of carbides on the border dendrites and dendritic cells; the carbides solidified as the first of the liquid in the form of dendrites; the carbides which have irregularly shape and size (size of the carbide was in range 3-15 μm). Matrix of the carbides consists of the plates α phase and β phase. Fracture toughness of titanium alloys is very dependent on microstructural and also crystallographic characteristics. The fracture of alloy after conventional heat treatment, similarly to fracture after remelting with GTAW is characterized by extremely fine dimples of plastic deformation. In the alloyed specimens the intergranular and crystalline fracture was identified.

References

[1] Cao X., Jahazi X., Cao M., M. Jahazi (2009). Effect of welding speed on butt joint quality of Ti–6Al–4V alloy welded using a high-power Nd:YAG laser. *Optics and Lasers in Engineering. 47*, 1231-1241.

[2] Garbacz H., Wieciński P., Ossowski M., Ortore M.G., Wierzchoń T., Kurzydłowski K.J. (2008). Surface engineering techniques used for improving the mechanical and tribological properties of the Ti6A14V alloy. *Surface & Coatings Technology. 202,* 2453-2457.

[3] Yong L., Shiron G., Hongtao L., Zhongmin J. (2009). Microstructure analysis and wear behavior of titanium cermet femoral head with hard TiC layer. *Journal of Biomechanics. 42*, 2708-2711.

[4] Filip R., Sieniawski J. (2006). Mikrostruktura i właściwości użytkowe warstwy wierzchniej stopu tytanu Ti-6Al-4V kształtowanej metodą stopowania laserowego. *Inżynieria Materiałowa 3*.

[5] Filip R. (2006). Alloying of surface layer of the Ti-6Al-4V titanium alloy through the laser treatment. *Journal of Achievements in Materials and Manufacturing Engineering. 15*, 174-180.

[6] Lisiecki A, Klimpel A. (2008). Diode laser surface modification of, Ti6Al4V alloy Ti improve erosion wear resistance. *Archives of Materials Science and Engineering. 32*, 5-12.

[7] Liqun L., Dejian L., Yanbin Ch., Chunming W., Fuquan L. (2009). Electron microscopy study of reaction layers between single-crystal WC particle and Ti–6Al–4V after laser melt injection. *Acta Materialia. 57*, 3606-3614.

[8] Ossowska A., Zielinski A., Buczek M. (2010). Influence of Laser Melting on Surface Layer Properties of Titanium Alloy Ti6Al4V. *Journal of Biomechanic. 43* (1), 55.

[9] Dudek A., Bałaga Z. (2009). Residual stress state in titanium alloy remelted using GTAW method. *Archives of Foundry Engineering. 9* (2), 193-196.

[10] Pleshakov E., Sienyav'ski Ya., Filip R. (2002). Laser surface modification of Ti-6Al-4V alloy with silicon carbide. *Materials Science. 38* (5), 646-651.

[11] Saresh N., Gopalakrishna Pillai M., Mathewa J. (2007). Investigations into the effects of electron beam welding on thick Ti–6Al–4V titanium alloy. *Journal of Materials Processing Technology. 192–193*, 83–88.

[12] Yuan-Ching L., Yu-Chi L. (2011). Microstructure and tribological performance of Ti–6Al–4V cladding with SiC powder. *Surface & Coatings Technology. 205*, 5400-5405.